A Blind I/Q Imbalance Compensation Technique for Direct-Conversion Digital Radio Transceivers

Josias Jacobus de Witt and Gert-Jan van Rooyen, *Member, IEEE*

***Abstract*—Although the quadrature mixing radio front-end offers an attractive way to perform frequency translation, its image-rejection capability is severely affected by the gain and phase imbalances (I/Q imbalances) between its two analog signal paths. Digital signal processing techniques have widely been proposed to compensate for these mixer imperfections. Of these techniques, the class of blind compensation techniques seems very attractive since no test signals are required. This paper presents a novel I/Q imbalance extraction technique that uses a Cholesky decomposition of the received signal's covariance matrix to extract the exact imbalances of the front-end. An analysis is also presented on extracting and separating the imbalances of a cascaded imbalanced modulator and demodulator. Both a block-based and an adaptive variant of the technique are proposed, and a performance evaluation over multipath channels is presented.**

***Index Terms*—Direct-conversion transceivers, I/Q imbalance compensation, quadrature imbalance compensation, radio communication equipment.**

I. Introduction

Quadrature mixing radio front-ends offer an attractive architecture to accomplish the direct modulation of digital signals due to their compact implementation and low cost [1], [2]. However, the image-rejection capabilities of practical quadrature mixing front-ends are deteriorated by the gain and phase imbalances (I/Q imbalances) between their two signal paths [3], [4].

Manuscript received May 7, 2007; revised November 13, 2007, March 13, 2008, May 21, 2008, and July 14, 2008. First published September 9, 2008; current version published April 22, 2009. This work was supported by Telkom SA through the Telkom Centre of Excellence. The review of this paper was coordinated by Prof. M. Juntti.

The authors are with the Department of Electrical and Electronic Engineering, Stellenbosch University, Stellenbosch 7600, South Africa (e-mail: gvrooyen@sun.ac.za).

Digital Object Identifier 10.1109/TVT.2008.2005414

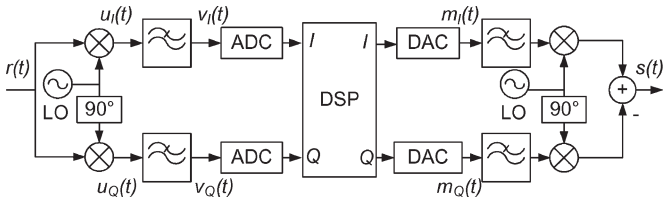

Fig. 1. Architecture of a quadrature modulator and demodulator.

Many authors have proposed digital signal processing techniques to compensate for these I/Q imbalances. Of these, the so-called "blind techniques" are particularly attractive since they avoid the test signals by extracting the imbalances from real data and usually require no extra calibration hardware. Blind methods that involve second-order statistics are often considered attractive due to their relatively low implementation complexity compared with methods such as blind source separation (BSS) [5]. Windisch and Fettweis [5] propose a technique that is suitable for low-IF receivers: the I/Q imbalances are extracted from the averages of N samples, but both the desired and image signals must be mixed down to 0 Hz. In [6], a block-averaging method termed "stat" is proposed, which extracts the I/Q imbalances by assuming that the I and Q channels are independent and have an equal mean power. Valkama *et al.* [7] propose a whitening transform (which is based on the eigenvalue decomposition) that can be implemented either in block form or adaptively. This transform decorrelates the I and Q signals but introduces an additional unknown rotation-reflection effect on the whitened signal, which needs to be resolved. In [8], a method similar to [5] is proposed, which is applicable to both low-IF and zero-IF receivers. This method uses block averages to extract the complex image rejection ratio (IRR). When used for compensation, this leaves an unknown amplitude scaling and phase rotation on the compensated signal.

The main contribution of this paper is a computationally efficient, blind I/Q compensation technique that targets inaccuracies across the full transmitter–receiver system and extracts the actual I/Q impairments. The proposed method relies on the knowledge of the second-order statistics of the received signal and uses a Cholesky decomposition of the received signal's covariance matrix to extract the I/Q imbalances. Unlike the methods of [5] and [9], this method is applicable to both zero-IF and low-IF transceivers. This technique not only aims to decorrelate the I and Q signals, as is done in [7] and [8], but also extracts the exact I/Q imbalance parameters, thus leaving no unknown rotation reflection in the compensated signal. It can adaptively be implemented and does not rely on block averaging, which enables imbalance tracking over time. An analysis is presented on the effect of noise, a frequency-selective channel, and a frequency offset between the transmitter and receiver local oscillators (LOs). It is then demonstrated that the I/Q compensation can effectively be combined with multipath equalization.

II. System Modeling

A. Quadrature Modulator

In Fig. 1, the basic architecture of a quadrature modulator and demodulator is shown. Let α_I and α_Q denote the gain of the I and Q channels of the quadrature mixer in the modulator. The gain imbalance is given by $\alpha_M = \alpha_I/\alpha_Q$. The phase imbalance of the modulator is defined as $\phi_M = \phi_I - \phi_Q$, where ϕ_I and ϕ_Q are the phase offsets

of the in-phase and quadrature components of the complex LO signal relative to an arbitrary reference.

The unbalanced complex oscillator at the modulator $x_M(t)$ can thus be written as

$$x_M(t) = \alpha_I \cos(2\pi\omega_c t + \phi_I) + j\alpha_Q \sin(\omega_c t + \phi_Q). \quad (1)$$

There may also exist nonzero dc offsets in the I and Q signal paths, which are denoted by κ_I and κ_Q for the respective channels, and a carrier leak-through component $\eta\cos(\omega_c t + \gamma)$.

Using the vector notation of [3], the complex baseband equivalent representation of the output of the unbalanced modulator, which is denoted by $\tilde{s}(t)$,[1] can be written as

$$\widetilde{\boldsymbol{s}}(t) = \boldsymbol{M}\,[\boldsymbol{m}(t) + \boldsymbol{a}] + \boldsymbol{b} \quad (2)$$

where we have defined

$$\begin{aligned} \boldsymbol{m}(t) &= [\, m_I(t) \quad m_Q(t)\,]^T \\ \boldsymbol{a} &= [\, \kappa_I \quad \kappa_Q\,]^T \\ \boldsymbol{b} &= [\, \eta\cos(\gamma) \quad \eta\sin(\gamma)\,]^T \\ \boldsymbol{M} &= \begin{bmatrix} \alpha_I\cos(\phi_I) & -\alpha_Q\sin(\phi_Q) \\ \alpha_I\sin(\phi_I) & \alpha_Q\cos(\phi_Q) \end{bmatrix}. \end{aligned} \quad (3)$$

$m(t) = m_I(t) + jm_Q(t)$ denotes the complex-valued baseband message signal. The choice of a suitable phase reference will be further discussed in Section III.

B. Demodulator

Similar to the discussion for the imperfect quadrature modulator, we may define the amplitude and phase imbalance of the demodulator as $\beta_D = \beta_I/\beta_Q$ and $\varphi_D = \varphi_I - \varphi_Q$, respectively. The imbalanced demodulator's complex quadrature oscillator signal can then be written, relative to the oscillator signal of the modulator, as

$$\begin{aligned} x'_D(t) = {} & \beta_I\cos(\omega_c t + \varphi_I + \Delta\omega t + \theta) \\ & - j\beta_Q\sin(\omega_c t + \varphi_Q + \Delta\omega t + \theta). \end{aligned} \quad (4)$$

The $\Delta\omega t + \theta$ terms inside the sine and cosine functions of (4) represent the difference in frequency and phase, respectively, between the modulator and demodulator's oscillators. Let the unwanted dc offset terms in the two signal paths be given by χ_I and χ_Q, and let a carrier leak-through component be given by $\xi\cos(\omega_c t + \Delta\omega t + \theta + \rho)$. If the two matched low-pass filters are employed to remove the double-frequency components, then the resultant signal at the output of the imbalanced demodulator $v(t)$ can be written in vector form (similar to [3]) as

$$\boldsymbol{v}(t) = \boldsymbol{D}\,[\boldsymbol{R}\tilde{\boldsymbol{r}}(t) + \boldsymbol{d}] + \boldsymbol{e} \quad (5)$$

where we have defined

$$\begin{aligned} \tilde{\boldsymbol{r}}(t) &= [\, \tilde{r}_I(t) \quad \tilde{r}_Q(t)\,]^T \\ \boldsymbol{d} &= [\, \xi/2\cos(\rho) \quad \xi/2\sin(\rho)\,]^T \\ \boldsymbol{e} &= [\, \chi_I \quad \chi_Q\,]^T \\ \boldsymbol{R} &= \begin{bmatrix} \cos(\Delta\omega t + \theta) & \sin(\Delta\omega t + \theta) \\ -\sin(\Delta\omega t + \theta) & \cos(\Delta\omega t + \theta) \end{bmatrix} \\ \boldsymbol{D} &= \begin{bmatrix} \beta_I\cos(\varphi_I) & \beta_I\sin(\varphi_I) \\ -\beta_Q\sin(\varphi_Q) & \beta_Q\cos(\varphi_Q) \end{bmatrix}. \end{aligned} \quad (6)$$

In (5), $\tilde{r}(t)$ represents the low-pass complex representation of the bandpass signal at the input to the demodulator.

C. Cascaded Effect in Digital Modulation Systems

Let a complex constellation point in an alphabet of M symbols be represented by a 2×1 vector $\boldsymbol{m}$. Using the results in Section II, we can write the expression for the received symbol, after the cascaded effect of the modulator and the demodulator's I/Q imbalances, as

$$\boldsymbol{v} = \boldsymbol{D}\,[\boldsymbol{R}(\boldsymbol{M}\boldsymbol{m} + \boldsymbol{c}) + \widetilde{\boldsymbol{n}}] + \boldsymbol{f} \quad (7)$$

where the dc terms $\boldsymbol{c} = \boldsymbol{M}\boldsymbol{a} + \boldsymbol{b}$, and $\boldsymbol{f} = \boldsymbol{D}\boldsymbol{d} + \boldsymbol{e}$. The noise vector $\widetilde{\boldsymbol{n}}$ is assumed to derive from two zero-mean independent and identically distributed (i.i.d.) random processes.

III. I/Q Imbalance Extraction

A. Demodulator Compensation

As in [6], an intentional frequency offset between the LO frequencies of the modulator and demodulator is used to separate the effect of their imbalances in the received signal. This offset causes the rotation matrix $\boldsymbol{R}$ in (7) to become time variant and results in a constant rotation of the signal constellation at the receiver. When the signal constellation is observed over an integer multiple of a 2π rotation, the rotation will diagonalize the covariance matrix of $\boldsymbol{R}(\boldsymbol{M}\boldsymbol{m} + \boldsymbol{c})$ in (7). In addition, since the components of the noise vector $\widetilde{\boldsymbol{n}}$ are considered to be independent, the covariance matrix of $\boldsymbol{R}(\boldsymbol{M}\boldsymbol{m} + \boldsymbol{c}) + \widetilde{\boldsymbol{n}}$ in (7) will be a diagonal matrix when observed over a multiple of 2π rotation of $\boldsymbol{R}$. Let $\boldsymbol{C} = \mathrm{diag}[\sigma^2\ \sigma^2]$ denote the covariance matrix of $\boldsymbol{R}(\boldsymbol{M}\boldsymbol{m} + \boldsymbol{c}) + \widetilde{\boldsymbol{n}}$. The resultant covariance matrix of $\boldsymbol{v}$ can then be written in terms of $\boldsymbol{C}$ as

$$\boldsymbol{C}' = \boldsymbol{D}\boldsymbol{C}\boldsymbol{D}^T. \quad (8)$$

Any symmetric positive-definite matrix $\boldsymbol{A} \in \mathbb{R}^{n\times n}$ can uniquely be factorized as $\boldsymbol{A} = \boldsymbol{G}\boldsymbol{G}^T$, where $\boldsymbol{G} \in \mathbb{R}^{n\times n}$ is a unique lower-triangular matrix (e.g., see [11, pp. 141]). This is known as the Cholesky factorization of $\boldsymbol{A}$. Since the covariance matrix $\boldsymbol{C}$ will be a diagonal matrix with positive entries, it is also a symmetric positive-definite matrix [11, pp. 140]. In this case, the positive definiteness of $\boldsymbol{C}'$ only depends on the distortion matrix $\boldsymbol{D}$. If $\boldsymbol{D}$ has full rank, then $\boldsymbol{C}'$ will necessarily be positive definite [11, pp. 140]. $\boldsymbol{D}$ will always have full rank unless $\varphi_D = \pm\pi/2$ or $\beta_D = 0$. When $\boldsymbol{C}'$ can be assumed to be symmetric and positive definite, we can define the Cholesky factorization of $\boldsymbol{C}'$ as

$$\boldsymbol{C}' = \boldsymbol{H}\boldsymbol{H}^T \quad (9)$$

where $\boldsymbol{H} \in \mathbb{R}^{2\times 2}$ is a unique lower-triangular matrix. Using (8) and the fact that $\boldsymbol{C}$ is assumed to be a diagonal matrix, we can write $\boldsymbol{C}'$ as

$$\boldsymbol{C}' = \boldsymbol{D}\boldsymbol{C}^{1/2}(\boldsymbol{C}^{1/2}\boldsymbol{D})^T. \quad (10)$$

[1]The baseband or low-pass equivalent of the passband signal $s(t)$ is defined as $\tilde{s}(t) = [s(t) + j\hat{s}(t)]e^{-j\omega_c t}$ [10, pp. 51], where $\hat{s}(t)$ denotes the Hilbert transform of $s(t)$.

The distortion matrix $\boldsymbol{D}$ can be modeled as a lower-triangular matrix by using the I channel as a reference in (6). When the I channel's phase is used as the reference phase, then $\varphi_I = 0$, and $\varphi_Q = -\varphi_D$. The distortion matrix $\boldsymbol{D}$ thus becomes

$$\boldsymbol{D} = \beta_I \begin{bmatrix} 1 & 0 \\ 1/\beta_D \sin(\varphi_D) & 1/\beta_D \cos(\varphi_D) \end{bmatrix}. \tag{11}$$

Using this result and the uniqueness of the Cholesky factorization, (9) and (10) imply that

$$\boldsymbol{H} = \boldsymbol{D}\boldsymbol{C}^{1/2} = \sigma \boldsymbol{D} \tag{12}$$

if we use the I channel as a reference. Since σ (on the diagonal of $\boldsymbol{C}$) is generally not known in a practical system, the imbalances φ_D and β_D must be extracted from $\boldsymbol{H}$ as

$$\varphi_D = \tan^{-1}\left(\frac{[\boldsymbol{H}]_{21}}{[\boldsymbol{H}]_{22}}\right) \tag{13}$$

$$\beta_D = \frac{\sqrt{[\boldsymbol{H}]_{21}^2 + [\boldsymbol{H}]_{22}^2}}{[\boldsymbol{H}]_{11}} \tag{14}$$

where $[\boldsymbol{H}]_{ij}$ is the jth element in the ith row of $\boldsymbol{H}$. The compensation for the quadrature imbalances of the demodulator is now performed by using the parameters obtained in (12) and (13) to compute the inverse of $\boldsymbol{D}$. The inverse of $\boldsymbol{H}$ could also be used as the compensation matrix, thus avoiding the computational complexity of computing (12) and (13). The effect will be a scaling of the signal space of $1/\sigma$, which can be lumped with the unknown channel gain.

B. Modulator Compensation

Once the imbalances of the demodulator are extracted and compensated for, we can attribute the remaining imbalances to the modulator. The conventional methods can now be used to accomplish a carrier phase synchronization, which inverts the effect of the rotation matrix $\boldsymbol{R}$. Assuming a perfect compensation of the demodulator imbalance matrix $\boldsymbol{D}$, the dc offset vector $\boldsymbol{f}$ (its estimation is a byproduct of covariance estimation), and the rotation matrix $\boldsymbol{R}$, the demodulated signal becomes

$$\boldsymbol{R}^{-1}\boldsymbol{D}^{-1}(\boldsymbol{v} - \boldsymbol{f}) = \boldsymbol{M}\boldsymbol{m} + \boldsymbol{c} + \boldsymbol{R}^{-1}\widetilde{\boldsymbol{n}}. \tag{15}$$

For modulator compensation, we consider digital modulation schemes with a signal space constellation that is symmetrical about both the real and imaginary axes after any offset from the origin is removed. We also assume that each of the M symbols in the symbol alphabet is equally probable to be transmitted. The covariance matrix $\boldsymbol{Y}$ of the constellation points $\boldsymbol{m}$ in the M-symbol alphabet (the signal space constellation) will then be a 2×2 diagonal matrix $\boldsymbol{Y} = \mathrm{diag}[\lambda_I^2 \ \lambda_Q^2]$. The covariance matrix of the noiseless signal space constellation after modulator imbalances is then $\boldsymbol{Y}' = \boldsymbol{M}\boldsymbol{Y}\boldsymbol{M}^T$. Since $\boldsymbol{Y}'$ exactly has the same form as $\boldsymbol{C}'$ in (10), a similar imbalance-extraction procedure to that used for the demodulator can be used to extract the modulator imbalances. In this case, the distortion matrix $\boldsymbol{M}$ can be modeled as a lower-triangular matrix by using the Q channel as a reference. Compensation for the quadrature imbalances of the modulator is now performed by using the I/Q imbalance parameters to compute the inverse of $\boldsymbol{M}$ and relaying this information as the control data back to the modulator to be applied there.

C. Demodulator Special Case

Consider the case where only an imbalanced demodulator is used (this is the assumption for almost all the references in Section I). The expression for the received signal can then be written as $\boldsymbol{v} = \boldsymbol{D}\boldsymbol{R}\boldsymbol{m}$, where we have now ignored the dc offset and noise terms without loss of generality. If we assume that the I and Q components of $\boldsymbol{m}$ are uncorrelated and have equal mean power (this is true for all rectangular quadratic-amplitude modulation (QAM), M-phase-shift keying (PSK) ($M > 2$) and orthogonal frequency-division multiplexing (OFDM) multicarrier signals [7]), then the covariance matrix of the source signal $\boldsymbol{m}$ is given by $\boldsymbol{Z} = \mathrm{diag}[\eta^2/2 \ \eta^2/2]$, where η^2 denotes the variance of $\boldsymbol{m}$. This results in the covariance matrix

$$\boldsymbol{Z}' = \boldsymbol{D}\boldsymbol{Z}\boldsymbol{D}^T = \eta^2/2\boldsymbol{D}\boldsymbol{D}^T \tag{16}$$

since the rotation matrix $\boldsymbol{R}$ has the property $\boldsymbol{R}\boldsymbol{R}^T = \boldsymbol{I}$. The performance of the extraction techniques presented in this paper is, therefore, independent of phase and frequency synchronization, as well as the specific modulation type, as long as the preceding assumptions hold.

D. Adaptive Algorithm

In practice, the distorted covariance matrices $\boldsymbol{C}'$ and $\boldsymbol{Y}'$ can be estimated by using sample averages over the N received symbols (the block-based approach). Alternatively, the Cholesky decomposition of the covariance matrix of the received signal can adaptively be computed without explicitly computing the covariance matrix. One such algorithm is given as [12]

$$\boldsymbol{y}(\boldsymbol{k}) = \boldsymbol{W}(\boldsymbol{k})\boldsymbol{x}(\boldsymbol{k}) \tag{17}$$

$$\boldsymbol{W}(\boldsymbol{k}+\boldsymbol{1}) = (1+\mu)\boldsymbol{W}(\boldsymbol{k}) - \mu \cdot \mathrm{tril}\left[\boldsymbol{y}(\boldsymbol{k})\boldsymbol{y}^{\boldsymbol{T}}(\boldsymbol{k})\right]\boldsymbol{W}(\boldsymbol{k}). \tag{18}$$

In the foregoing algorithm, k denotes the iteration, $\boldsymbol{x}$ denotes the input sample, μ denotes the positive step size, and tril() takes the lower-triangular matrix of its argument. $\boldsymbol{W}$ is the 2×2 adapted matrix; in this case, $\boldsymbol{W}$ denotes the inverse of the Cholesky factorization of the covariance matrix of $\boldsymbol{x}$. $\boldsymbol{W}$, therefore, already represents the compensation matrix, and no further inversion is required. This approach is attractive since it has a low computational complexity and enables the adaptive tracking of I/Q imbalances over time. It is also more memory efficient than a block-based approach.

IV. Practical Performance Issues

A. Sensitivity to LO Frequency Offset

In practice, the exact value of the LO frequency offset (which is used to isolate the demodulator imbalances from that of the modulator) may not be known. In addition, when this frequency offset is normalized with respect to the symbol sampling rate, it will almost certainly result in an irrational number due to the lack of frequency coherence between the transmitter and receiver LOs. The combined rotation and symbol sampling will then produce an aperiodic sampling sequence. It is, therefore, unlikely that the rotating symbol space will be observed over an exact multiple of a 2π rotation in practice. However, as the number of symbols used in the imbalance estimation is increased to include many cycles of the approximate 2π constellation rotation, the residual estimation error diminishes. This is verified in Simulation 1 (Section V).

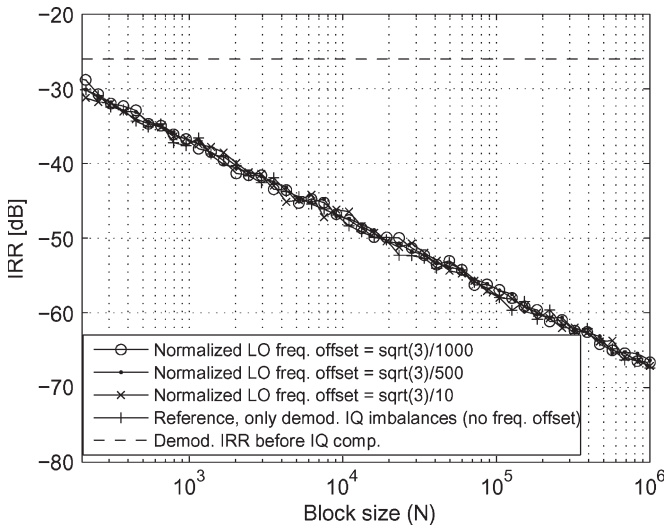

Fig. 2. IRR of an imbalanced 64-QAM demodulator after compensation, indicating the insensitivity of the modulator–demodulator imbalance-isolation process toward the LO frequency offset. The imbalance parameters were $\alpha_M = \beta_D = 1.05$ (0.42 dB) and $\phi_M = \varphi_D = 5^\circ$ (IRR of -26 dB).

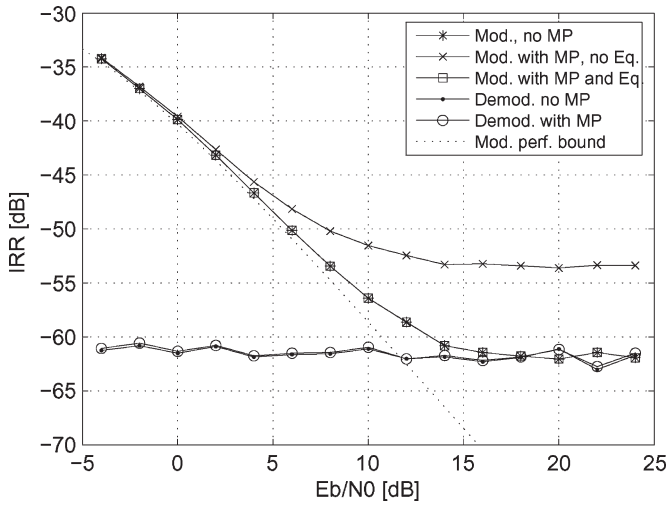

Fig. 3. Effectiveness of the modulator imbalance compensation (in terms of IRR at the modulator after compensation) on a 16-QAM system over a noisy multipath (MP) channel with and without channel equalization (Eq.). The imbalance parameters were $\alpha_M = 1.05$ (0.42 dB) and $\phi_M = 5^\circ$ (IRR of -26 dB). The multipath channel $h = [0.8660 + 0.5000i \quad 0.0643 + 0.0766i \quad 0.0098 - 0.0017i]$. The dotted line indicates the performance bound when extracting the imbalance parameters from a diagonally loaded covariance matrix (see text). The demodulator performance in the presence of the same channel is also shown.

B. Effect of Noise

From (14), it can be seen that the i.i.d. channel noise term $(\boldsymbol{R}^{-1}\tilde{\boldsymbol{n}})$ will cause a diagonal loading on the covariance matrix of the signal space $\boldsymbol{Mm}$, introducing an estimation error in the modulator compensation parameters. The reliability of the modulator imbalance extraction is consequently a function of the signal-to-noise ratio (SNR), as confirmed in Simulation 2 (Section V-B). Analogous to the modulator case, any noise entering the system after the demodulator will also have the same detrimental effect on the demodulator compensation performance. However, the signal plus channel noise power entering the demodulator is usually much larger than the noise introduced after the demodulator, thus rendering its effect on performance negligible.

C. Effect of a Frequency-Selective Channel

From (7), the effect of a frequency-selective channel may be included in the cascaded system

$$\boldsymbol{v}(t) = \boldsymbol{D}\left[\boldsymbol{R}(t)\boldsymbol{h}(t) * \{\boldsymbol{Mm}(t) + \boldsymbol{c}\} + \widetilde{\boldsymbol{n}}\right] + \boldsymbol{f} \tag{19}$$

where $\boldsymbol{h}(t)$ is the channel's complex impulse response, and $*$ is the convolution operator. Since the LO frequency offset will still serve to diagonalize the covariance matrix of $\boldsymbol{h}(t) * \{\boldsymbol{Mm}(t) + \boldsymbol{c}\}$, the frequency-selective channel will not affect the demodulator imbalance extraction performance.

Consider the demodulator special case in Section III-C, i.e., $\boldsymbol{v}(t) = \boldsymbol{DRh}(t) * \boldsymbol{m}(t)$ (where an LO frequency offset is not necessarily assumed). When a signal with initially uncorrelated I and Q components with equal variance passes through a complex frequency-selective channel, the output's components will also be uncorrelated [7]. Since this is the assumption in Section III-C, we may conclude that the frequency-selective channel will also have no effect in this case. This is confirmed in Simulations 3 and 5 (Section V).

For modulator imbalance extraction, the observable signal will be $\boldsymbol{h}(t) * \boldsymbol{Mm}(t)$. If the effect of the channel is thus not removed before imbalance extraction, it will distort the compensation parameters. Although there is a strong connection between the I/Q imbalances and the channel equalization performance, Rykaczewski *et al.* [13] argue that the demodulator imbalances will affect the channel equalization process more than the modulator imbalances. Since an LO frequency offset allows us to extract and compensate for demodulator imbalances independent of the channel, we can expect the remaining effect of modulator impairments on the channel equalization to be small. This statement is further studied in Simulation 2 (Section V).

V. Simulation Results

A. Simulation 1: Sensitivity to the LO Frequency Offset

Fig. 2 illustrates the insensitivity of the modulator–demodulator imbalance isolation process to the LO frequency offset. An imbalance extraction was performed using the block-based approach. A 64-QAM system with $\alpha_M = \beta_D = 1.05$ and $\phi_M = \varphi_D = 5^\circ$ was simulated at an SNR per bit (SNR/bit or E_b/N_0) of 15 dB. Irrational numbers were chosen for the LO frequency offsets in the simulations to mimic the noncoherent frequency references of the independent transmitters and receivers. The IRR of the demodulator defined as [3]

$$\text{IRR} = \frac{\beta_D^2 + 1 - 2\beta_D\cos(\varphi_D)}{\beta_D^2 + 1 + 2\beta_D\cos(\varphi_D)} \tag{20}$$

was used as the performance benchmark. As a reference, the case of no modulator imbalances (and, therefore, also no LO frequency offset) is also shown. Note that the precision to which the demodulator imbalances can be isolated and estimated, when an imbalanced modulator is also present, is insensitive to the LO frequency offset and its 2π rotation of the signal space when a sufficient number of symbols is used in the estimation, since no noticeable performance degradation could be observed when compared with the reference.

B. Simulation 2: Effect of the Communication Channel

Fig. 3 shows the effects of the channel SNR and multipath propagation on the compensated IRR performance of a modulator and demodulator. A 16-QAM system was simulated. First, the imbalanced

modulator's imbalances ($\alpha_M = 1.05$, $\phi_M = 5^\circ$) were extracted at a perfect demodulator after the signal had passed through a noisy multipath channel ($h[n] = [0.866 + 0.5i \quad 0.0643 + 0.0766i \quad 0.0098 - 0.0017i]$ with symbol spacing) with and without channel equalization. Channel equalization was performed by using a zero-forcing equalizer (ZFE) (see, e.g., [14, pp. 661]). Second, the extraction performance of an imbalanced demodulator ($\beta_D = 1.05$, $\varphi_D = 5^\circ$) was investigated by using the same channel, with the data generated by a perfect modulator. Both modulator and demodulator imbalances were extracted by using the block-based approach with $N = 5 \cdot 10^5$. In addition, we show the performance bound obtained when the theoretical covariance matrix of the signal constellation, which was distorted by the modulator I/Q imbalances and diagonally loaded with values equal to the noise variance, is subjected to the Cholesky factorization process.

As expected, the diagonal loading caused by the channel noise affects the modulator performance but not that of the demodulator. At high SNR, the multipath effects dominate the modulator performance but have no effect on the demodulator. When channel equalization is performed before the modulator imbalances are estimated, the loss in compensation performance can be regained. After the channel equalization, the modulator performance, like that of the demodulator, is dominated by the number of symbols used in the imbalance estimation process at high SNR. A comparison with Fig. 2 at $N = 5 \cdot 10^5$ also demonstrates the compensation technique's insensitivity toward the specific modulation scheme assuming a symmetrical constellation.

C. Simulation 3: BER Performance

The performance of the proposed technique was evaluated in a cascaded imbalanced modulator and demodulator scenario, where the coupling effect of the modulator and demodulator imbalances was removed with the use of a normalized LO frequency offset of $\sqrt{3}/500$ rad/symbol. No effort was made to ensure an observation period of an exact 2π rotation. Fig. 4 shows the bit error rate (BER) performance of 64-QAM in an additive white Gaussian noise (AWGN) channel with perfect synchronization and symbol timing. Imbalance values of $\alpha_M = \beta_D = 1.05$ and $\phi_M = \varphi_D = 5^\circ$ were introduced. The imbalance estimation using the block-based approach was performed at various noise levels and then used for compensation at that noise level. The imbalances of the modulator were extracted at the receiver and compensated for at the transmitter. The number of symbols used to estimate the imbalances N is also shown. The technique improves the BER to the reference level (no I/Q imbalances) for the cases of $N = 10^4$ and $N = 10^5$ and manages to significantly improve the BER performance even for $N = 10^3$.

Fig. 5 shows a more realistic scenario for 64-QAM. In this figure, a noisy multipath channel with impulse response $h[n] = [0.9962 + 0.0872i \quad 0.0643 + 0.0766i \quad 0.0492 - 0.0087i]$ (symbol period spacing) was simulated. Nyquist filters with a rolloff factor of 0.5 were used, and a symbol timing error of 5% was introduced. A zero-forcing channel equalization was performed after the demodulator I/Q compensation. The proposed technique again recovers the performance loss due to the I/Q imbalances to the level of the reference system (no I/Q imbalances).

D. Simulation 4: Comparison to Other Methods

The performance of the proposed technique was compared to two other techniques from the literature that used second-order statistics in a block-based estimation, i.e., the technique of Anttila *et al.* [8] and the "stat" method of [6]. The three methods all have comparable

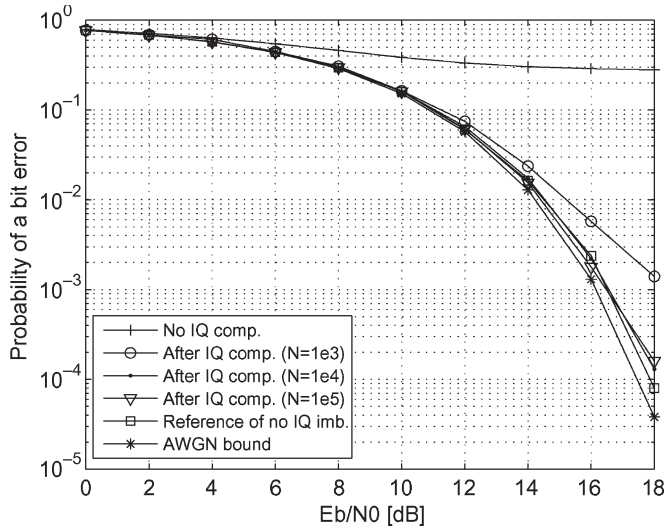

Fig. 4. BER performance of 64-QAM in an AWGN channel, $\alpha_M = \beta_D = 1.05$ (0.42 dB), and $\phi_M = \varphi_D = 5^\circ$. The normalized LO frequency offset was $\sqrt{3}/500$ rad/symbol.

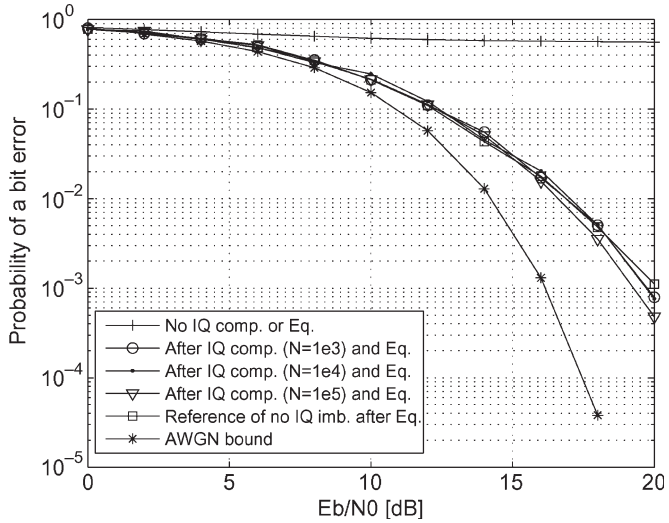

Fig. 5. BER performance of 64-QAM in a multipath channel ($h = [0.9962 + 0.0872i \quad 0.0643 + 0.0766i \quad 0.0492 - 0.0087i]$) with a symbol timing error of 5% and imbalances of $\alpha_M = \beta_D = 1.05$ (0.42 dB) and $\phi_M = \varphi_D = 5^\circ$. The normalized LO frequency offset was $\sqrt{3}/500$ rad/symbol. The BER performance is shown before I/Q compensation (IQ comp.) or channel equalization (Eq.), as well as after I/Q compensation with different values of N. As a reference, the system performance without any I/Q imbalances is also shown.

computational complexities. In the experiment, an imbalanced receiver ($\beta_D = 1.05$ and $\varphi_D = 5^\circ$) was used with 64-QAM modulation. The symbol rate was defined to be 3.84 MHz at an RF center frequency of 2 GHz. A multipath fading channel was used with a power delay profile following the Vehicular A model [15] and a mobility of 100 km/h. No frequency synchronization was performed at the receiver, and the normalized LO frequency offset was $\sqrt{3}/1000$ rad/symbol. The compensation parameters were estimated for various SNR/bit values. These parameters were then used to determine the IRR capability of the receiver after compensation at that SNR/bit. The IRR before compensation was -26 dB. Fig. 6 shows the average of 1000 runs. All three techniques essentially perform equally well, and their performance is not severely affected by the nonidealities introduced in the simulation. It is also shown that the performance

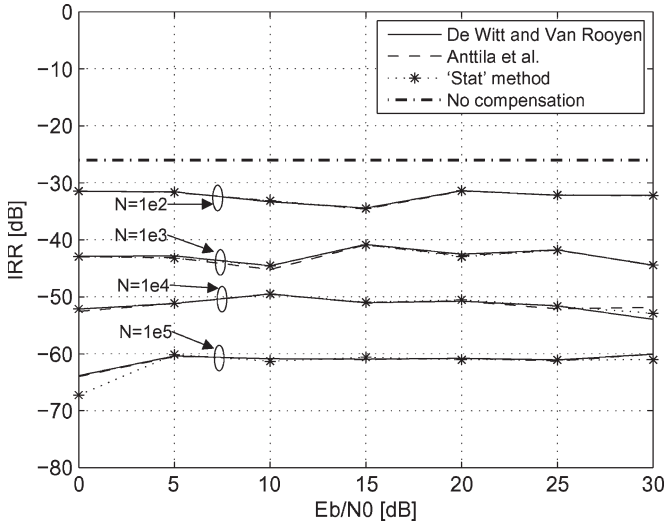

Fig. 6. Comparison of the image-suppression capabilities of the proposed technique with that of Anttila *et al.* [8] and the "stat" method of [6]. The received signal was 64-QAM with a normalized LO frequency offset of $\sqrt{3}/1000$ rad/symbol in a fading multipath channel defined by the Vehicular A model [15] with 100-km/h mobility. The receiver imbalances are $\beta_D = 1.05$ (0.42 dB) and $\varphi_D = 5^\circ$ (IRR of -26 dB). N denotes the block size used during estimation.

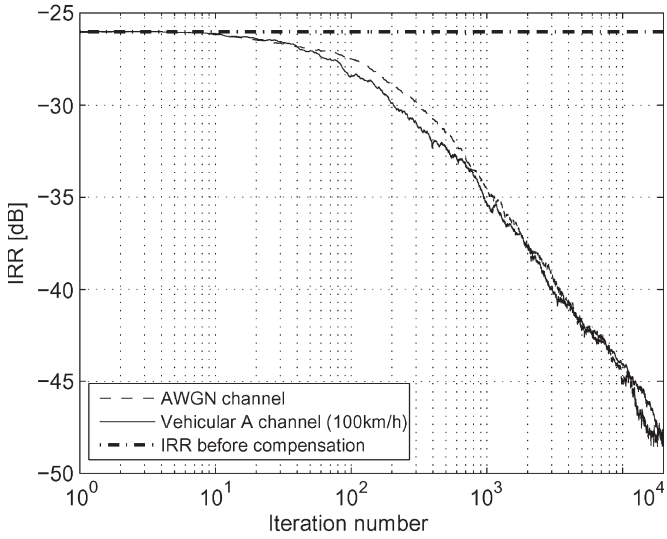

Fig. 7. Performance of the adaptive version of the proposed technique. The received signal was 64-QAM with an LO frequency offset of $\sqrt{3}/1000$ rad/symbol. A fading multipath channel that is defined by the Vehicular A model [15] with 100-km/h mobility was used. The SNR/bit was 15 dB with receiver I/Q imbalances of $\beta_D = 1.05$ (0.42 dB) and $\varphi_D = 5^\circ$ (IRR of -26 dB). The step size was $\mu = 0.0001$.

of the technique presented in this paper is indeed independent of the frequency synchronization.

E. Simulation 5: Adaptive Algorithm Performance

Finally, the adaptive (iterative) version of the proposed technique (Section III-D) was tested on an imbalanced ($\beta_D = 1.05$ and $\varphi_D = 5^\circ$) demodulator using 64-QAM modulation. The channel and mobility parameters were chosen to be the same as for Simulation 4. A frequency offset of $\sqrt{3}/1000$ rad/symbol was used with an SNR/bit of 15 dB. Fig. 7 shows the convergence performance of the iterative algorithm that is expressed in terms of the IRR performance of the demodulator after compensation and averaged over 100 runs. As a comparison, the simulation was repeated without the multipath fading channel. It is seen that the compensation performance remains unaffected by the fading multipath channel.

VI. Conclusion

This paper has introduced a novel blind-compensation technique to correct the I/Q imbalances that are inherent to practical quadrature mixing transceivers, based on the knowledge of the second-order statistics of the received signal. Unlike other techniques, the proposed technique not only aims to decorrelate the I and Q signals but extracts exact gain and phase imbalances through a Cholesky decomposition of the received signal's covariance matrix as well. A low-complexity adaptive version of the proposed method has also been presented. It was shown analytically and through simulation that the proposed technique's performance is inherently independent of the frequency and phase offsets when the original signal's real and imaginary components are uncorrelated and of equal power. The simulation results indicate that the proposed technique manages to restore the implementation loss in BER due to quadrature imbalances, even for high-order modulation schemes, in a multipath environment.

References

[1] R. Marchesani, "Digital precompensation of imperfections in quadrature modulators," *IEEE Trans. Commun.*, vol. 48, no. 4, pp. 552–556, Apr. 2000.
[2] G. Xing, M. Shen, and H. Liu, "Frequency offset and I/Q imbalance compensation for direct-conversion receivers," *IEEE Trans. Wireless Commun.*, vol. 4, no. 2, pp. 673–680, Mar. 2005.
[3] J. K. Cavers and M. W. Liao, "Adaptive compensation for imbalance and offset losses in direct conversion transceivers," *IEEE Trans. Veh. Technol.*, vol. 42, no. 4, pp. 581–588, Nov. 1993.
[4] B. Razavi, "Design considerations for direct-conversion receivers," *IEEE Trans. Circuits Syst. II, Analog Digit. Signal Process.*, vol. 44, no. 6, pp. 428–435, Jun. 1997.
[5] M. Windisch and G. Fettweis, "Blind I/Q imbalance parameter estimation and compensation in low-IF receivers," in *Proc. 1st ISCCSP*, Hammamet, Tunisia, Mar. 2004, pp. 75–78.
[6] P. Rykaczewski and F. Jondral, "Blind I/Q imbalance compensation in multipath environments," in *Proc. ISCAS*, New Orleans, LA, May 2007, pp. 29–32.
[7] M. Valkama, M. Renfors, and V. Koivunen, "Blind signal estimation in conjugate signal models with application to I/Q imbalance compensation," *IEEE Signal Process. Lett.*, vol. 12, no. 11, pp. 733–736, Nov. 2005.
[8] L. Anttila *et al.*, "Blind moment estimation techniques for I/Q imbalance compensation in quadrature receivers," in *Proc. IEEE PIMRC*, Helsinki, Finland, 2006, pp. 2611–2614.
[9] M. Windisch and G. Fettweis, "Standard-independent I/Q imbalance compensation in OFDM direct-conversion receivers," in *Proc. 9th InOWo*, Dresden, Germany, 2004.
[10] J. G. Proakis and M. Salehi, *Communication Systems Engineering*, 2nd ed. Englewood Cliffs, NJ: Prentice–Hall, 2002.
[11] G. H. Golub and C. F. van Loan, *Matrix Computations*, 2nd ed. Baltimore, MD: Johns Hopkins Univ. Press, 1989.
[12] S. C. Douglas, "Simple adaptive algorithms for Choleski, LDT^T, QR, and eigenvalue decompositions of autocorrelation matrices for sensor array data," in *Proc. Conf. Rec. 35th Asilomar Conf. Syst. Comput.*, 2001, vol. 2, pp. 1134–1138.
[13] P. Rykaczewski, M. Valkama, and M. Renfors, "On the connection of I/Q imbalance and channel equalization in direct-conversion transceivers," *IEEE Trans. Veh. Technol.*, vol. 57, no. 3, pp. 1630–1636, May 2008.
[14] J. G. Proakis, *Digital Communications*, 4th ed. Boston, MA: McGraw-Hill, 2001.
[15] *Guidelines for the Evaluation of Radio Transmission Technologies for IMT-2000*, 1997. Recommendation ITU-R M.1225.